Summary

Introduction

Rapid environmental change, IPCC, estimated temperature rise.

Trend to precocity in plants, flowering time, etc. Advance in phenology.

Problem: Understanding (and predicting?) long-lived plant adaptation to climate change

Based on previously developed demographic and quantitative genetics model (see), added fluctuating environments. Made theoretical predictions. Estimated fluctuations using data from phenological data (PHENOFIT).

Materials and Methods

Population model

We used a previously developed model with stage-structure (Sandell 2014, master's thesis). We considered a population of trees split in two classes, immature (I) and mature (M). only mature individuals reproduce. Each year, an immature individual can survive with a probability s_I, mature and reproduce with a probability of m. At the same time, a mature individual has a probability s_M to survive. First-time reproducers, i.e. immature that became mature and reproduce the same year, have a fecundity of f_1, while experienced reproducers, those who already reproduced at least once, have a fecundity of f_2. Produced seeds have a probability s_0 to survive and join the pool of immature trees. The standard parameters set is given in (Table 1). The population census is just before reproduction. The population dynamics can be predicted using the following matrix (Caswell, 2001):

$$A = \begin{pmatrix} a_{II} & a_{IM} \\ a_{MI} & a_{MM} \end{pmatrix} = \begin{pmatrix} s_0 m f_1 + s_I(1-m) & s_0 f_2 \\ s_M m & s_M \end{pmatrix} \tag{1}$$

, where a_{ij}, the transition rate, describes the contribution of stage j individuals to stage i the next year. With given initial conditions we can compute the number of individuals in the two stages by iterating matrix multiplication by A.

We implemented density-dependence in this population, so that the population would not continuously increase (see Figure 1). We assumed seed germination and survival parameter s_0 declined with increasing density of mature and immature competitors using a Beverton-Holt function to avoid chaotic behaviors (Caswell, 2001):

$$s_0 = \frac{s_{0,max}}{1 + k_I N_I + k_M N_M} \tag{2}$$

with k_I and k_M the weights of immature (N_I) and mature (N_M) population respectively. $s_{0,max}$ is the maximum achievable s_0.

Phenotype and life-history traits

In this population we observed a single phenotype z: the bud-burst date. Here, bud-burst date is expressed in julian days (numbered days in the year, 1st of January being 1 in julian days). In our model, an individual is born with a given phenotype and keeps it throughout his life.

We supposed certain life-history traits for each individual - s_I immature survival, f_1 first reproducers fecundity and f_2 experienced reproducers - (see Equation 1) to be Gaussian function of phenotype z. Thus, bud-burst date directly influence their values. They can are expressed as follow:

$$\begin{cases} s_I(z) = s_I(\theta_s)\exp\left(-\dfrac{(z-\theta_s)^2}{2\omega_s}\right) \\ f_1(z) = f_1(\theta_f)\exp\left(-\dfrac{(z-\theta_f)^2}{2\omega_f}\right) \\ f_2(z) = f_2(\theta_f)\exp\left(-\dfrac{(z-\theta_f)^2}{2\omega_f}\right) \end{cases} \tag{3}$$

, θ_s is the optimal bud-burst date for survival, i.e. phenotype where s_I is at its maximum $s_I(\theta_s)$; ω_s is the width of the Gaussian function, its inversely related to selection intensity: with small ω_s values, only a restricted range of bud-burst dates would have important survival rates. f_1 and f_2 have similar expressions, but the optimal bud-burst date θ_f is different from θ_s, f_1 and f_2 only differ by their maximum values $f_i(\theta_f)$, with f_1 lower than f_2 (see Table 1 to have standard parameters values).

The optimal trait values θ_s and θ_f differ between stages and life-history components, but trait value does not change along the life of an individual, then there is a trade-off between the two fitness components. And the evolution of the trait affects the life-history of the individual.

If we want to compute mean transition rate $\overline{a_{ij}}$, we need to average s_I, f_1 and f_2 (ex: $\overline{a_{IM}} = s_0\overline{f_2}$):

$$\mathrm{E}[s_I] = \overline{s_I} = \int p_I(z)s_I(z)\,\mathrm{d}z \tag{4}$$

, with $p_I(z)$ the distribution of z in the immature stage, as we study a quantitative trait we suppose p_I has a Gaussian distribution with mean $\overline{z_I}$ and width P_I the phenotypic variance in the immature stage (Lande, 1982). We end with the following expression for $\overline{s_I}$:

$$\overline{s_I}(\overline{z_I}) = s_I(\theta_s)\sqrt{\frac{\omega_s}{\omega_s + P_I}}\exp\left(-\frac{(\overline{z_I}-\theta_s)^2}{2(\omega_s+P_I)}\right) \tag{5}$$

We obtain similar expressions for $\overline{f_1}$ and $\overline{f_2}$.

Iterations at each time step

Assuming the phenotype has a Gaussian distribution, the mean genotypic value of matures and immatures at the next time step is given by (Barfield et al. 2011 Eq.5) :

$$\overline{g_I}' = (c_{IM}\overline{g_M} + c_{II}\overline{g_I}) + (c_{IM}G_M\beta_{a_{IM}} + c_{II}G_I\beta_{a_{II}}) \tag{6a}$$
$$\overline{g_M}' = (c_{MI}\overline{g_I} + c_{MM}\overline{g_M}) + (c_{MI}G_I\beta_{a_{MI}} + c_{MM}G_M\beta_{a_{MM}}) \tag{6b}$$

with $c_{ij} = \frac{n_j\overline{a_{ij}}}{n_i'}$, the contribution of stage j individuals to next years pool of stage i individuals, as a fraction of i individuals at the next time step n_i'; and $\beta_{a_{ij}}$ the selection gradient as $\beta_{a_{ij}} = \frac{\partial \ln \overline{a_{ij}}}{\partial \overline{z}}$ (Barfield et al., 2011). The selection gradient represent the force of directional selection (Lande, 1982).

The first term is a weighted average of mean genotypes contributing to this stage; while the second shows the effect of selection.

To have the formal expressions of $\beta_{a_{ij}}$ we need to compute the selection gradients on life-history components:

$$\begin{aligned}\beta_{\overline{s_I}} &= \frac{\partial \ln \overline{s_I}}{\partial \overline{z_I}} &&= \frac{\theta_s - \overline{z_I}}{\omega_s + P_I} \\ \beta_{\overline{f_1}} &= \frac{\partial \ln \overline{f_1}}{\partial \overline{z_I}} &&= \frac{\theta_f - \overline{z_I}}{\omega_f + P_I} \\ \beta_{\overline{f_2}} &= \frac{\partial \ln \overline{f_2}}{\partial \overline{z_M}} &&= \frac{\theta_f - \overline{z_M}}{\omega_f + P_M}\end{aligned} \tag{7}$$

And because we have for example $\overline{a_{II}} = s_0 m \overline{f_1} + \overline{s_I}(1-m)$ we get the selection gradient:

$$\beta_{a_{II}} = \frac{s_0 m \overline{f_1} \beta_{\overline{f_1}} + \overline{s_I} \beta_{\overline{s_I}} (1-m)}{\overline{a_{II}}} \tag{8}$$

We have a similar recursion for phenotypes (Barfield et al., 2011). They depend on terms of direct transition of individuals from one stage to the other $\overline{t_{ij}}$ and events leadings to new individuals $\overline{f_{ij}}$ (and we have $\overline{a_{ij}} = \overline{t_{ij}} + \overline{f_{ij}}$):

$$\overline{z'_I} = c^t_{II}(\overline{z_I} + P_I \beta_{t_{II}}) + c^f_{II}(\overline{g_I} + G_I \beta_{f_{II}}) + c^f_{IM}(\overline{g_M} + G_M \beta_{f_{IM}}) \tag{9a}$$

$$\overline{z'_M} = c^t_{MI}(\overline{z_I} + P_I + \beta_{t_{MI}}) + c^t_{MM}(\overline{z_M} + P_M + \beta_{t_{MM}}) \tag{9b}$$

, with $\beta_{t_{II}}$ the gradient of selection defined as above in Equation 6a, i.e. $\beta_{t_{II}} = \frac{\partial \ln \overline{t_{II}}}{\partial \overline{z_I}}$; $c^t_{ij} = \frac{n_j \overline{t_{ij}}}{n'_i}$ the contribution by direct transition of stage j to stage i and $c^f_{ij} = \frac{n_j \overline{f_{ij}}}{n'_i}$ the contribution by birth.

Approximation under weak selection

Under weak selection, the mean phenotype at equilibrium in the population $\overline{z}$ follows in constant environment (Engen et al., 2011):

$$\overline{z_{eq}} = \frac{\gamma_f \theta_f + \gamma_s \theta_s}{\gamma_f + \gamma_s} \tag{10}$$

, with,

$$\gamma_f = \frac{v_I u_I s_0 m \overline{f_1}}{\lambda(P_I + \omega_f)} + \frac{v_I u_M \frac{G_M}{G_I} s_0 \overline{f_2}}{\lambda(P_M + \omega_f)} \tag{11a}$$

and

$$\gamma_s = \frac{v_I u_I \overline{s_I}(1-m)}{\lambda(P_I + \omega_s)} \tag{11b}$$

γ_f and γ_s represent the respective weight of each of the optimum in the trade-off between θ_f and θ_s for $\overline{z_{eq}}$. Indeed, if $\theta_f = \theta_s$ then $\overline{z_{eq}} = \theta_f = \theta_s$. But if $\theta_f \neq \theta_s$, then the mean phenotype on the trade-off depends on γ_f and γ_s and the ratio between them.

Fluctuating optimums

During my internship, I tried to mimic environmental fluctuations, by making the optima fluctuate as such:

$$\begin{cases} \theta_f(t) = \overline{\theta_f} + \alpha_f \xi_f \\ \theta_s(t) = \overline{\theta_s} + \alpha_s \xi_s \end{cases} \tag{12}$$

α_i is the sensitivity of θ_i to noise ξ_i. ξ_f and ξ_s are noise vectors drawn at each time step from a bi-variate normal distribution with respectively σ^2_f and σ^2_s variances and correlation ρ_N. Thus we get normal fluctuations, correlated with a correlation coefficient of ρ_N.

Under varying environment we get an another approximation under weak selection from (Engen et al., 2011) describing the change of mean phenotype:

$$\Delta\overline{z}(t) = -G_I\gamma(\overline{z}(t) - \theta_v(t)) \tag{13}$$

, with

$$\gamma = \gamma_f + \gamma_s \tag{14a}$$
$$\theta_v(t) = \overline{z_{eq}} + \xi_v \tag{14b}$$
$$\xi_v = \frac{\alpha_f\xi_f + \alpha_s\xi_s}{\alpha_f + \alpha_s} \tag{14c}$$

We see that the change in the mean phenotype depends on the sensitivity of the optima α_i as well as on the magnitude of the variations.

Trend in change

To model climate-change, and especially the trend to increase temperature with time, we included a trend in the variation of the optima. The optima still experience fluctuations as above they linearly vary with time:

$$\begin{cases} \theta_i(t) = \overline{\theta_i} + \alpha_i\epsilon(t) \\ \epsilon(t) = kt + \xi_i \end{cases} \tag{15}$$

With k having a negative value, the optima decrease with time.

Phenofit data

PHENOFIT is a phenology model including several sub-models, from environmental and phenological data it simulates the survival and reproduction of an average tree to predict its range (Morin et al., 2008).

We used output from PHENOFIT (simulations performed by A. Duputié) from 1950 to 2100 for the sessile oak (*Quercus petraea*) about predicted bud burst date and predicted fitnesses in 6 localities (see Figure 4). We had fitness predictions for phenotype around the modeled date (a range of 21 days). From these data we predicted the optima fluctuations. Considering fecundity f as a Gaussian function around this date with the same form as f_1 in Equation 5:

$$\beta = \frac{\partial \ln f}{\partial \overline{z}} = \frac{\theta_f - \overline{z}}{\omega_f + \sigma_z^2} \tag{16}$$

Using (Lande and Arnold, 1983), with z Gaussian, $p(z)$ the distribution of z in the population, $f(z)$ the fitness associated with z and $\overline{f}$ the mean fitness in the population, we computed selection gradients from PHENOFIT simulation outputs as::

$$\beta = \frac{\mathrm{cov}(z, \frac{f(z)}{\overline{z}})}{\sigma_z^2} \tag{17}$$

From (16) and (17) we can express θ_f:

$$\theta_f = \frac{\mathrm{cov}(z, \frac{f(z)}{\overline{z}})}{\sigma_z^2}(\omega_f + \sigma_z^2) + \overline{z} \tag{18}$$

In our estimations we considered $p(z)$ to be Gaussian around the modeled date by PHENOFIT, with a variance of $P_I = 40$ as in our analytic model. We normalized this distribution so that all dates in the population would be in the 42 days interval around the modeled date.

Trend analyses

All statistical analyses were made using R (R Core Team, 2014), graphics were drawn using ggplot2 (Wickham, 2009), data were handled using dplyr (Wickham and Francois, 2014).

To estimate the trend of the θ_f variations, we considered a trend model with three components: a general decreasing linear trend, a white noise component with a constant variance and a more dramatic noise leading to "catastrophic" events, with negative θ_f values.

The regular noise and the trend were estimated excluding those catastrophic events, we kept only value of θ_f over 60, which is the lower bound of the realizable range of bud burst date of oak trees. Then we performed a linear regression between values of θ_f and time, giving us an estimation of k from Equation 15. Analyzing the residuals gives us the variance of $\alpha_f \xi_f$ from the same equation.

Results

Constant environment and density-dependence

We used the previously developed model in (Sandell et al. 2014, master's thesis) and simulated (see Figure 1) a tree population for 150 years in a constant environment, with and without density-dependence on s_0, assess the effects of a more realistic demography.

As expected, density-dependence allow regulating the population (Figure 1 right panel), as the number of mature and immature individuals seem to converge respectively to 18000 and 10000 individuals, while without density-dependence the population is exponentially growing.

Looking at the phenotype, we started from exactly the same starting point $z = 116$ for phenotypic and genotypic values. Without density-dependence, the population quickly converge to the equilibrium phenotype ($\overline{z_{weak}}$ given by the approximation in Equation 10), $\overline{z_{weak}} = 116$ in this case. With density-dependence the equilibrium is shifted towards the survival optimum θ_s ($\overline{z_{weak,dd}} = 121.8$, $\theta_s = 130$ while $\theta_f = 100$).

The lower seed survival s_0 decreases γ_f (11a) changing the weights in (10), making it more interesting to favor the survival of already established immature trees than the production of many propagules with very little survival prospect.

Within the density-dependent model the mean immature phenotype $\overline{z_I}$ converge quicker than the mean mature phenotype $\overline{z_M}$ to the equilibrium. It is because of stage-structured nature of our model, the mature stage is a combination of individuals that lived for around 40 generations (given our life-cycle), it buffers adaptation. To make $\overline{z_M}$ closer to $\overline{z_{weak}}$, immature individuals with a phenotype closer to $\overline{z_{weak}}$ need to survive long enough to mature and outnumber initial mature individuals with phenotype further from $\overline{z_{weak}}$.

Fluctuating optima

To mimic a more realistic environment we made the optima fluctuate, with various correlations between them. We simulated three populations using the same random seed. We only vary correlations between noises.

Explain in the text correlation of z_I with $\theta_s(t)$

Trend in the environment

We implemented a decreasing trend in θ_f with fluctuations (Figure 3) to mimic climate change. We averaged values over 15 simulations for life-history traits while showed a single simulation for the phenotype (respectively bottom and top panels Figure 3).

Parameter	Notation	Value
Life Cycle		
Optimal phenotype for fecundity	θ_f	100
Optimal phenotype for immature survival	θ_s	130
Fecundity function width	ω_f	400
Survival function width	ω_s	400
Heritability	h^2	0.5
Phenotypic variance of immatures	P_I	40
Phenotypic variance of matures	P_M	40
Genotypic variance of immatures	$G_I = P_I \times h^2$	20
Genotypic variance of matures	G_M	20
Survival of immature at phenotypic optimum	$\overline{s_I}(\overline{z} = \theta_s)$	0.8
Fecundity of first time reproducers at optimum	$\overline{f_1}(\overline{z} = \theta_f)$	100
Fecundity of experienced reproducers at optimum	$\overline{f_2}(\overline{z} = \theta_f)$	200
Maturation rate of immature	m	0.02
Combined survival and germination rate of seed	s_0	0.03
Survival of mature stage	s_M	0.99
Density-dependence		
Maximum s_0 in density-dependence function	$s_{0,max}$	0.12
Decreasing factor due to immatures	k_I	0.001
Decreasing factor due to matures	k_M	0.005
Fluctuations		
Sensitivity of optimum for fecundity to fluctuation	α_f	5
Sensitivity of optimum for survival to fluctuation	α_s	5
Noise variance for fecundity	$\sigma^2_{\xi_f}$	3.725
Noise variance for survival	$\sigma^2_{\xi_s}$	3.725
Correlation between noises	ρ_N	0.5
Trend coefficient	k	-0.15

Table 1: Standard parameter set

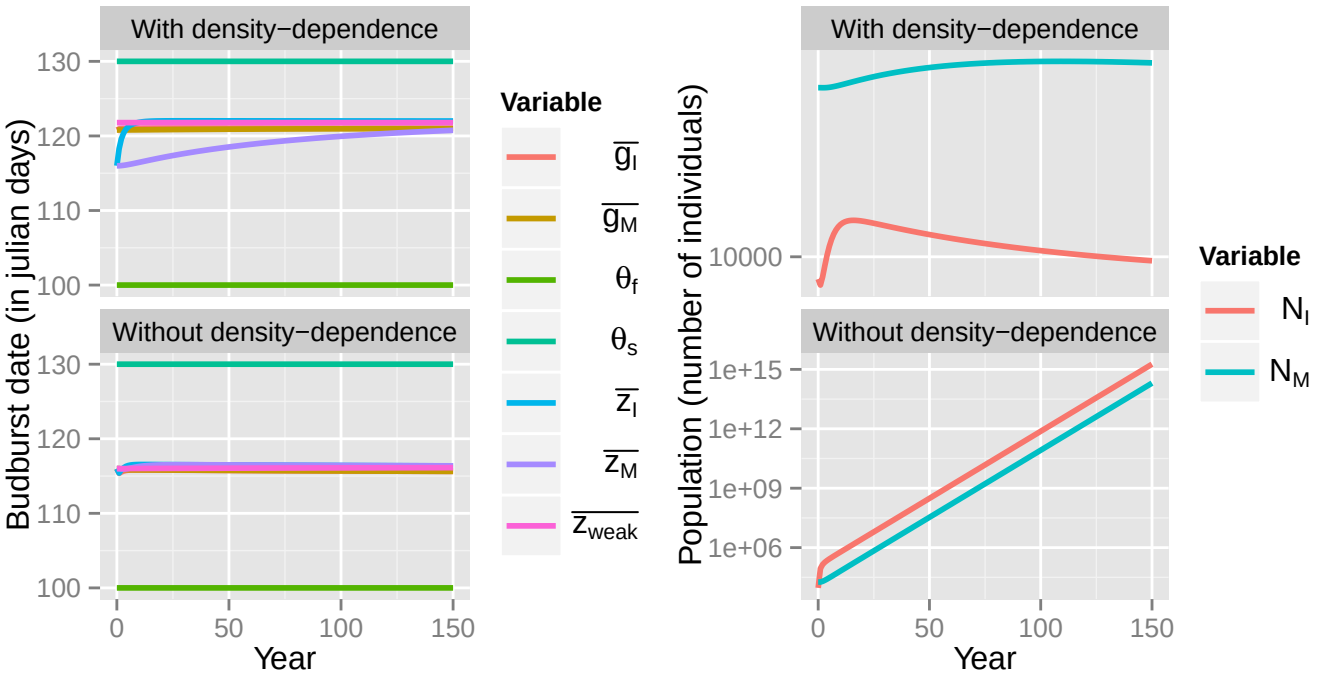

Figure 1: Effect of density-dependence on phenotypes and populations. **Left panel**: Phenotype variations in population ($\overline{z_I}, \overline{z_M}$) with their corresponding genotypic values ($\overline{g_I}, \overline{g_M}$) all starting from $z = 116$, and the approximation given by Equation 10; **right panel**: demography, number of immature individuals (N_I, red), number of mature individuals (N_M, blue). Starting from Stable-Stage Distribution (SSD) in constant environment, note the logarithmic scale used.

s_I has an interesting behavior, it first increases, reaches a maximum, then decreases. The decreasing trend in optima variation causes at first the mean population phenotype to move closer to θ_s, thus maximizing s_I values when it crosses θ_s line, as soon as it moves beyond s_I starts to decrease again. The fluctuations seem to decrease s_I (mean difference of 0.5), it may be a cost associated with the variance of optimum fluctuations, the optimum is often under the mean population value.

On the contrary f_1 and f_2 do not show a different pattern with or without fluctuations. They decrease because the mean population phenotype go further away from θ_f.

Seed germination and survival s_0 is increased by fluctuations, via an indirect mechanism: fluctuations decrease immature survival s_I, thus decreasing the immature population N_I and so the mature population N_M; this population decrease also decrease competition and density, increasing s_0 as it is density-dependent (see Equation 2).

As expected, the decreasing trend in θ_f creates a lag between the optima and the mean population values, because adaptation is slower than the rate of change. However, the population can still survive with such a rate if the difference between the optima and the means become constant. On a very long scale (2500 years) it is what happens in this case, the population maintain by changing its phenotype fast enough to track the optima variation (data not shown).

Estimation of the fluctuations

In 6 localities (map Figure 4 bottom left) using PHENOFIT output, we computed θ_f values at these locations (top 3 rows of Figure 4). For the 6 sites, predicted θ_f decrease with time, it is more precocious as time passes. This observation matches the advance of phenology observed in the literature because of climate change.

Over the general trend, we observe a small amplitude variation (with a standard deviation of 9.6 d), corresponding to year to year change in θ_f and some dramatic decreases in its values, sometimes reaching negative values (For example at BIC site in 1976). The frequency of these events increase

with time as they become common after 2050 for all sites. Note that those events are biased towards the decrease of θ_f, as there is no equivalent dramatic increases.

The negative values of θ_f computed in Figure 4, may seem striking as there is no such thing as a negative bud-burst date! It indicates strong directional selection to shorten bud-burst those years with very little sign of quadratic selection on that trait. As bottom right panel of Figure 4 shows, we can have negative value of θ_f and still have achievable phenotypes. If θ_f is very negative for a given year (less than -100 in 2048 for LAB), it means there will be no reproduction this year (flat tail of blue curve, bottom right oanel Figure 4).

We excluded those extreme events to estimate the trend in the variation of θ_f (see Materials and Methods). Using linear regression on θ_f with time, we found a rate of $-0.15\,\mathrm{d\,yr^{-1}}$, with normal residuals having a variance of 93.1 d^2 (data not shown, $R^2 = 0.2435$, $p = 1.185\text{e-}7$, $F = 32.5$ with 101 d.f.).

We investigated whether there was a break between years modeled from real data by PHENOFIT (before 2001) and years modeled using climate models with climate change included (from 2001). We performed the same regression as above, without taking apart the extreme values, for all sites, splitting the data before 2001 and from 2001. Taking all years, for each site.

Discussion

Difference in $\overline{z}$ and $\overline{g}$ with fluctuations because of selection on viability.

Increasing number of extreme events from predictions.

Authors Contributions and Acknowledgments

References

Barfield, M., Holt, R. D. and Gomulkiewicz, R. (2011). Evolution in Stage-Structured Populations (2 versions). The American Naturalist *177*, 397--409.

Caswell, H. (2001). Matrix population models : construction, analysis, and interpretation. Sinauer Associates.

Engen, S., Lande, R. and Sæther, B.-E. (2011). Evolution of a Plastic Quantitative Trait in an Age-Structured Population in a Fluctuating Environment. Evolution *65*, 2893--2906.

Lande, R. (1982). A Quantitative Genetic Theory of Life History Evolution. Ecology *63*, 607--615.

Lande, R. and Arnold, S. J. (1983). The Measurement of Selection on Correlated Characters. Evolution *37*, 1210--1226.

Morin, X., Viner, D. and Chuine, I. (2008). Tree species range shifts at a continental scale: new predictive insights from a process-based model. Journal of Ecology *96*, 784--794.

R Core Team (2014). R: A Language and Environment for Statistical Computing. R Foundation for Statistical Computing Vienna, Austria.

Wickham, H. (2009). ggplot2: elegant graphics for data analysis. Springer New York.

Wickham, H. and Francois, R. (2014). dplyr: A Grammar of Data Manipulation. R package version 0.3.0.2.

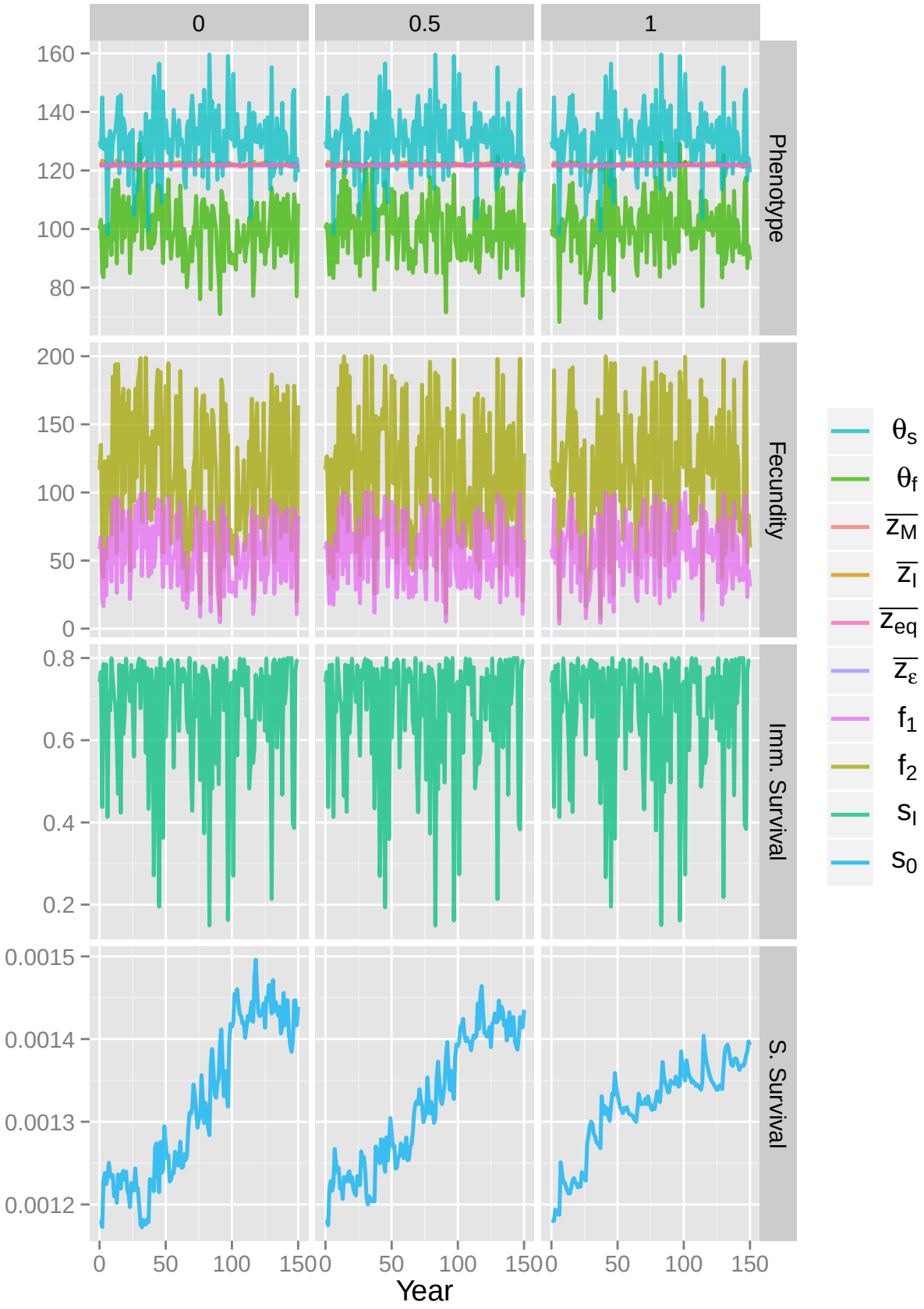

Figure 2: Effect of the correlation of fluctuations on phenotypes and life-history traits. Correlation coefficient ρ_N values of noises are indicated at the the top of each column. Phenotype and approximations are shown in julian days, $\overline{z_\epsilon}$ is the approximation from Equation 13. Mean fecundities are in number of seeds produced. The two bottom rows are survival rates, the top one is $\overline{s_I}$ the mean survival of immature individuals, the bottom one is s_0 the rate of survival and germination of seeds (see Materials and Methods).

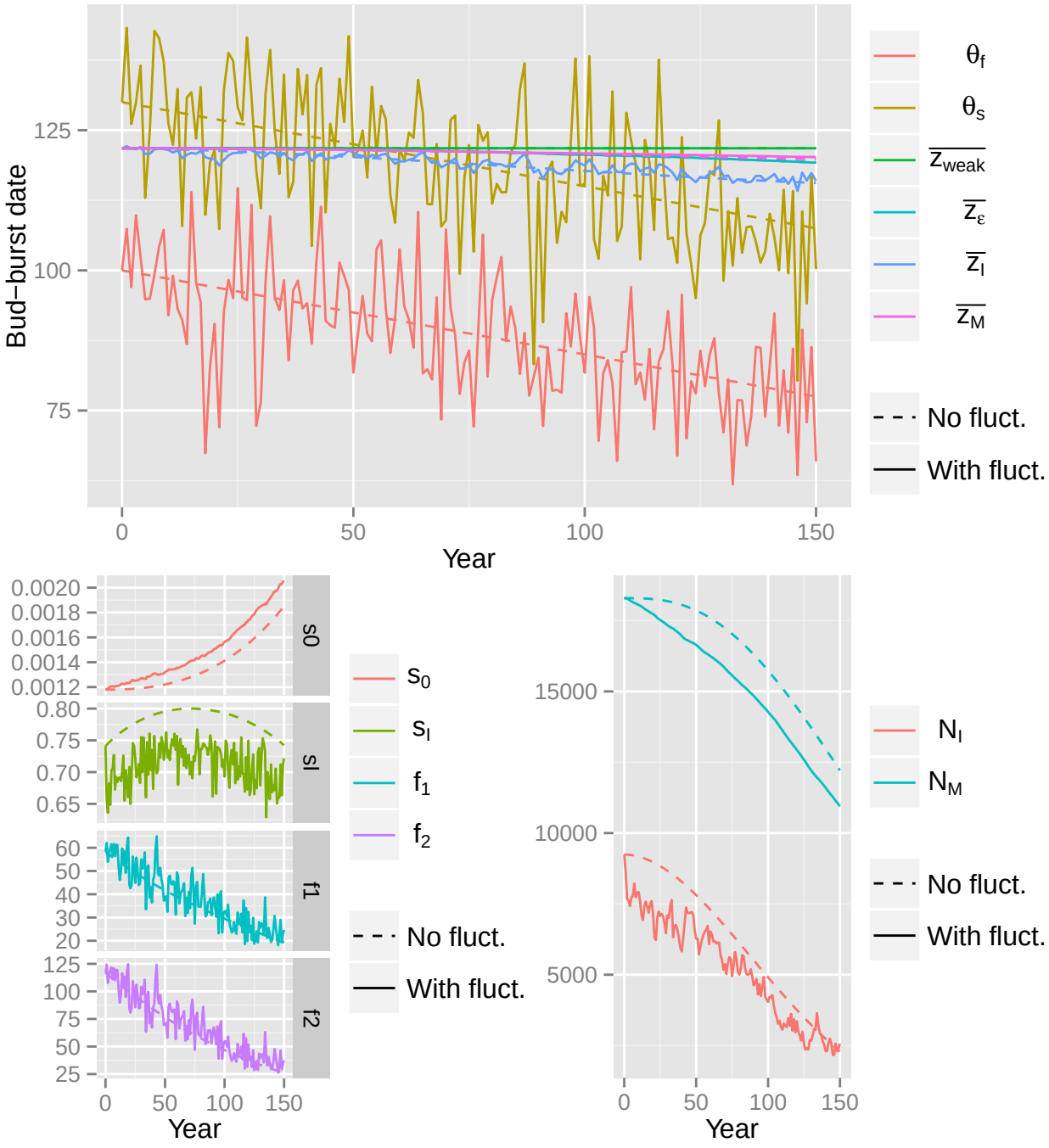

Figure 3: Mixed influences of trend and fluctuations on the population. **Top panel**: Phenotype evolution with and without fluctuations, results from a single simulation; **Bottom panel:** (**Left**) Life-History Traits evolution depending on fluctuations, survival are rates while fecundities are expressed in produced seeds; (**Right**) demography. **With fluct.**: fluctuating optima with a linear trend, **No fluct.** linearly decreasing optima. Results shown with fluctuations were averaged over 15 independent simulations for demography and life-history traits.

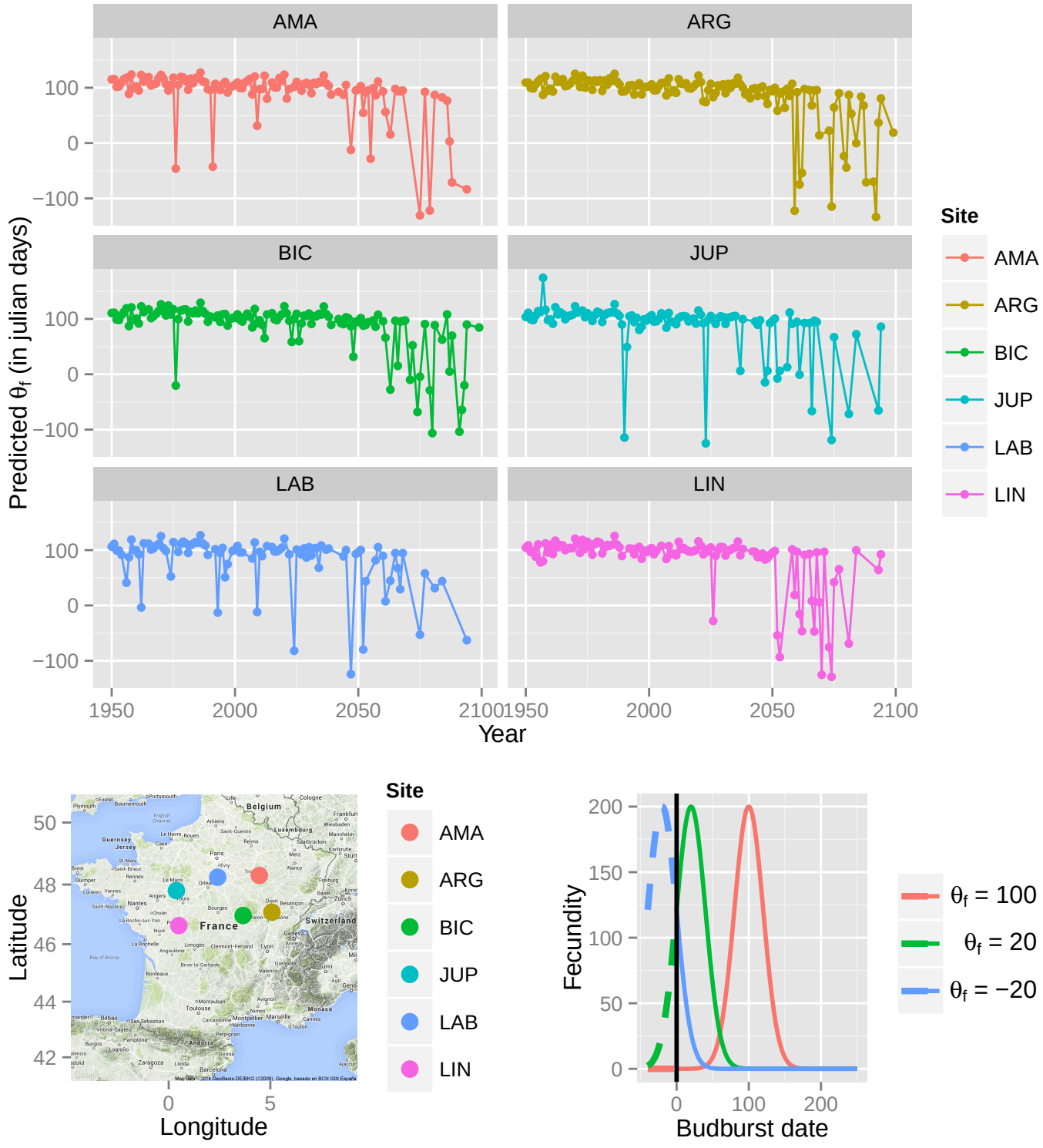

Figure 4: θ_f estimations from PHENOFIT data. Top 3 rows: estimations of θ_f for each study site see Materials and Methods for details. Bottom left panel: map of the study sites. Bottom right panel: Theoretical fecundity functions with parameters from Table 1 with values of θ_f equals to 100, 20 and -20, solid lines indicate achievable phenotype, dashed lines show theoretical curves but unreachable phenotypes.